

Article

Global Clear-Sky Aerosol Speciated Direct Radiative Effects over 40 Years (1980–2019)

Supplement

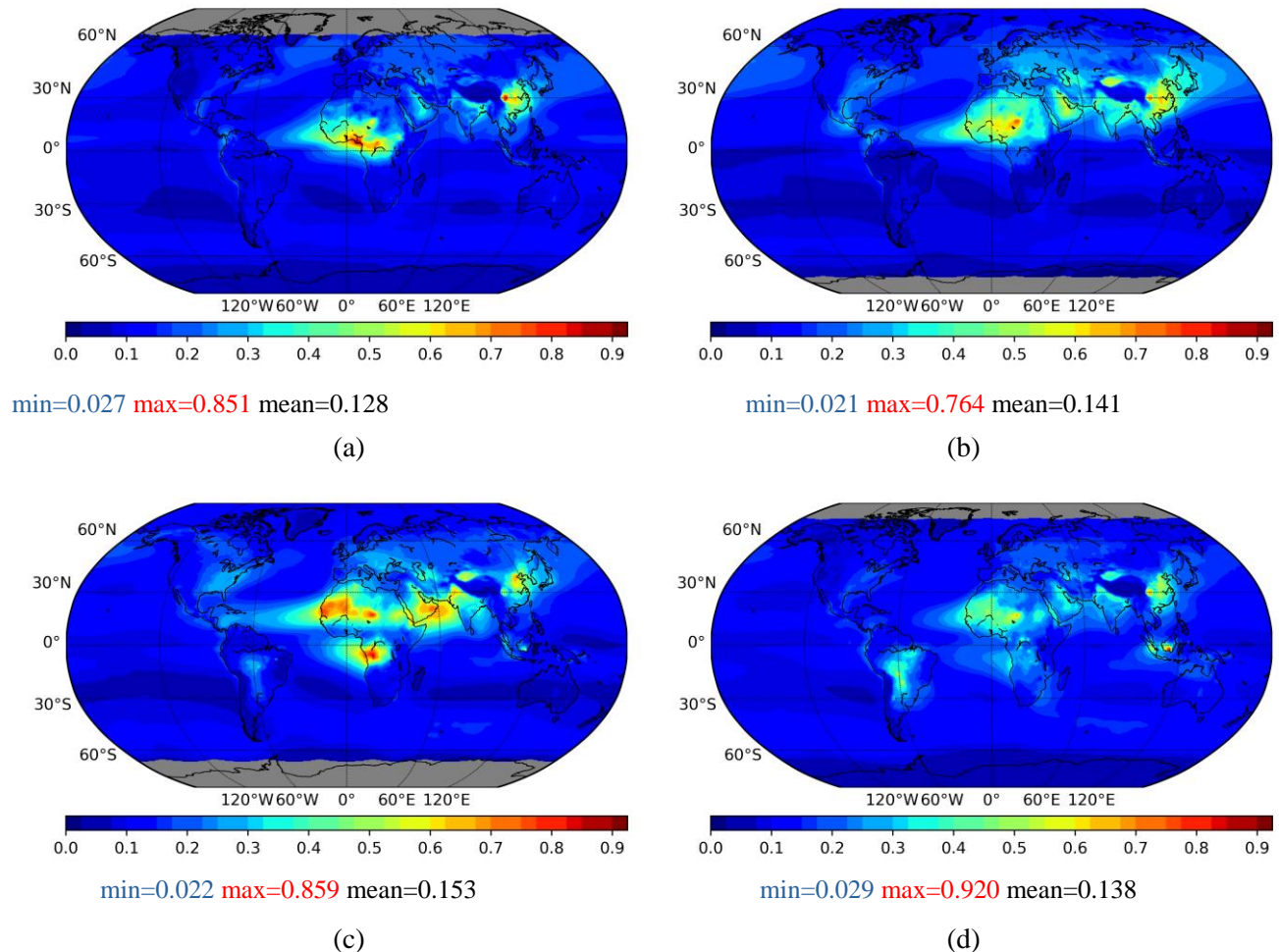


Figure S1i. Mean seasonal (1980–2019) global distribution of MERRA-2 Optical Depth at the wavelength of 550 nm for the total aerosol load. (a) winter, (b) spring, (c) summer, (d) autumn.

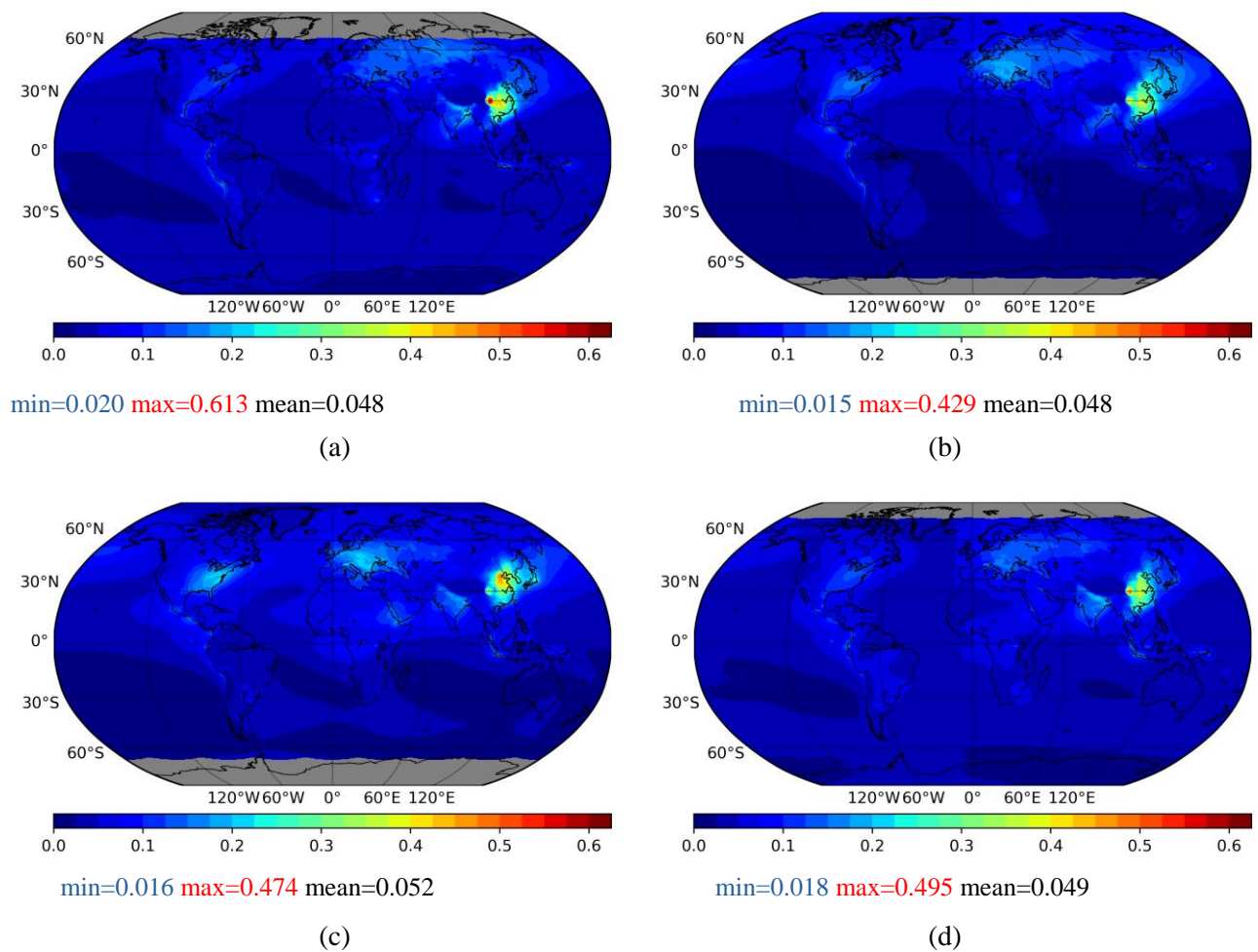


Figure S1ii. Mean seasonal (1980–2019) global distribution of MERRA-2 Optical Depth at the wavelength of 550 nm for sulfate particles. (a) winter, (b) spring, (c) summer, (d) autumn.

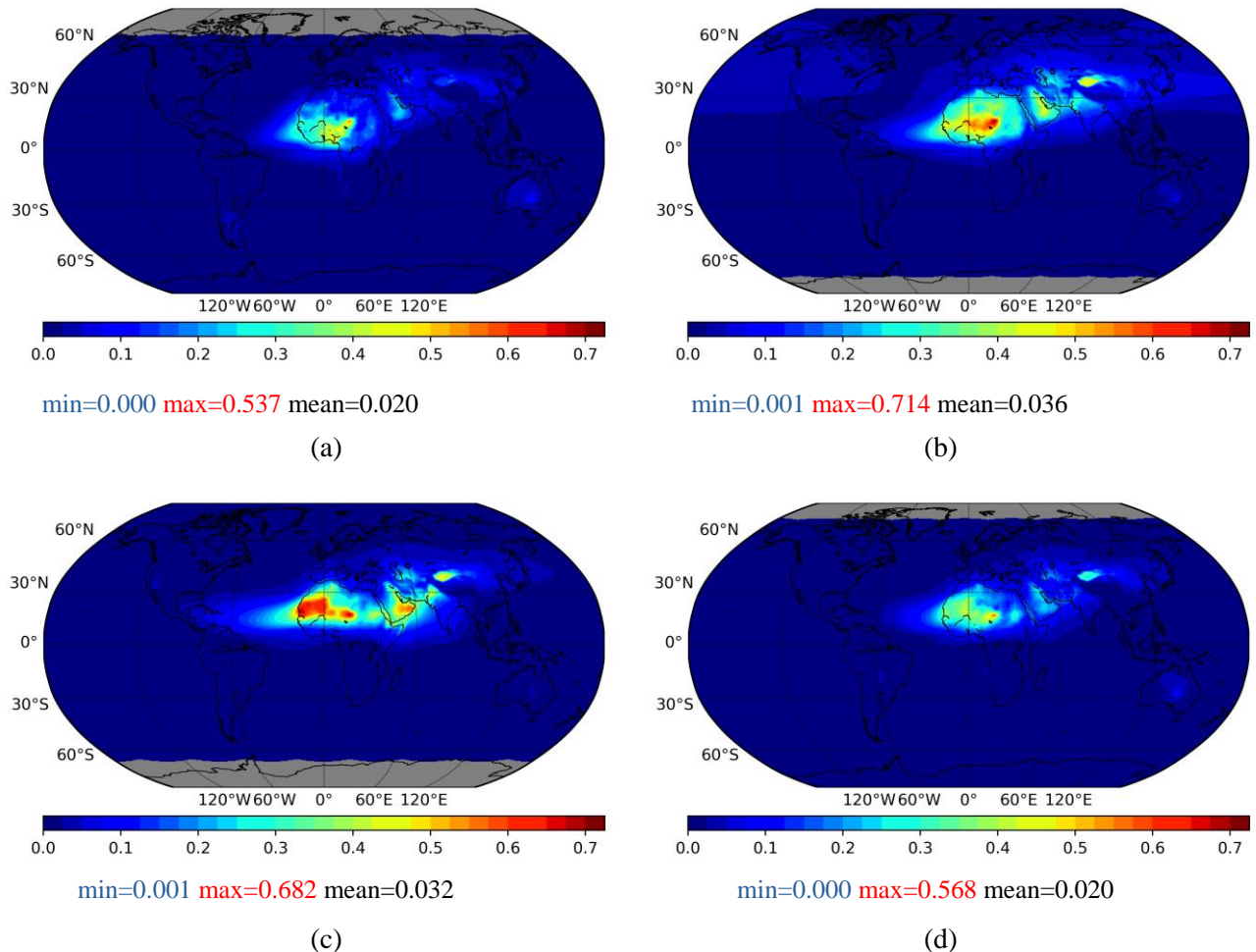


Figure S1iii. Mean seasonal (1980–2019) global distribution of MERRA-2 Optical Depth at the wavelength of 550 nm for dust particles. (a) winter, (b) spring, (c) summer, (d) autumn.

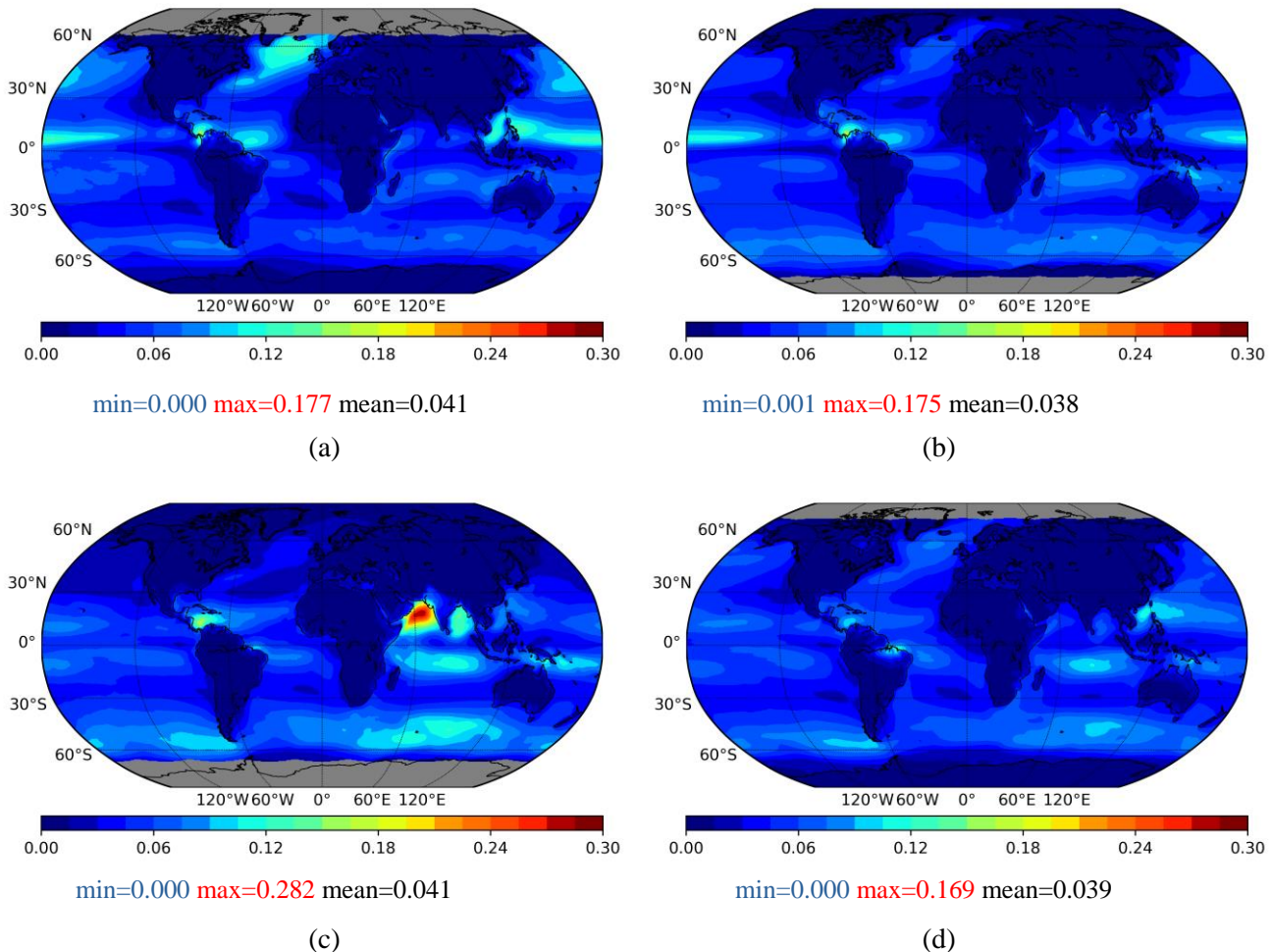


Figure S1iv. Mean seasonal (1980–2019) global distribution of MERRA-2 Optical Depth at the wavelength of 550 nm for dust particles. (a) winter, (b) spring, (c) summer, (d) autumn.

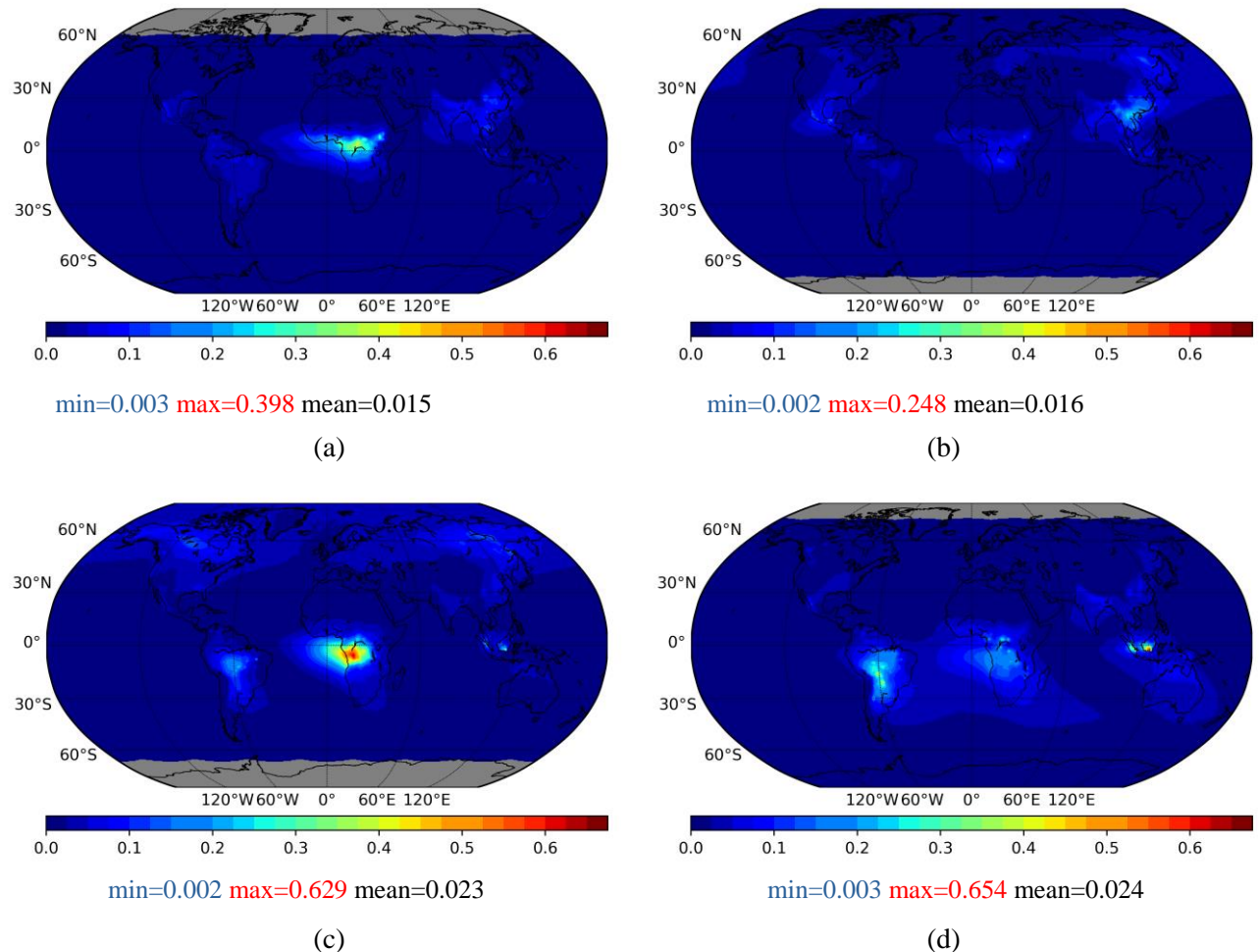


Figure S1v. Mean seasonal (1980–2019) global distribution of MERRA-2 Optical Depth at the wavelength of 550 nm for organic carbon particles. (a) winter, (b) spring, (c) summer, (d) autumn.

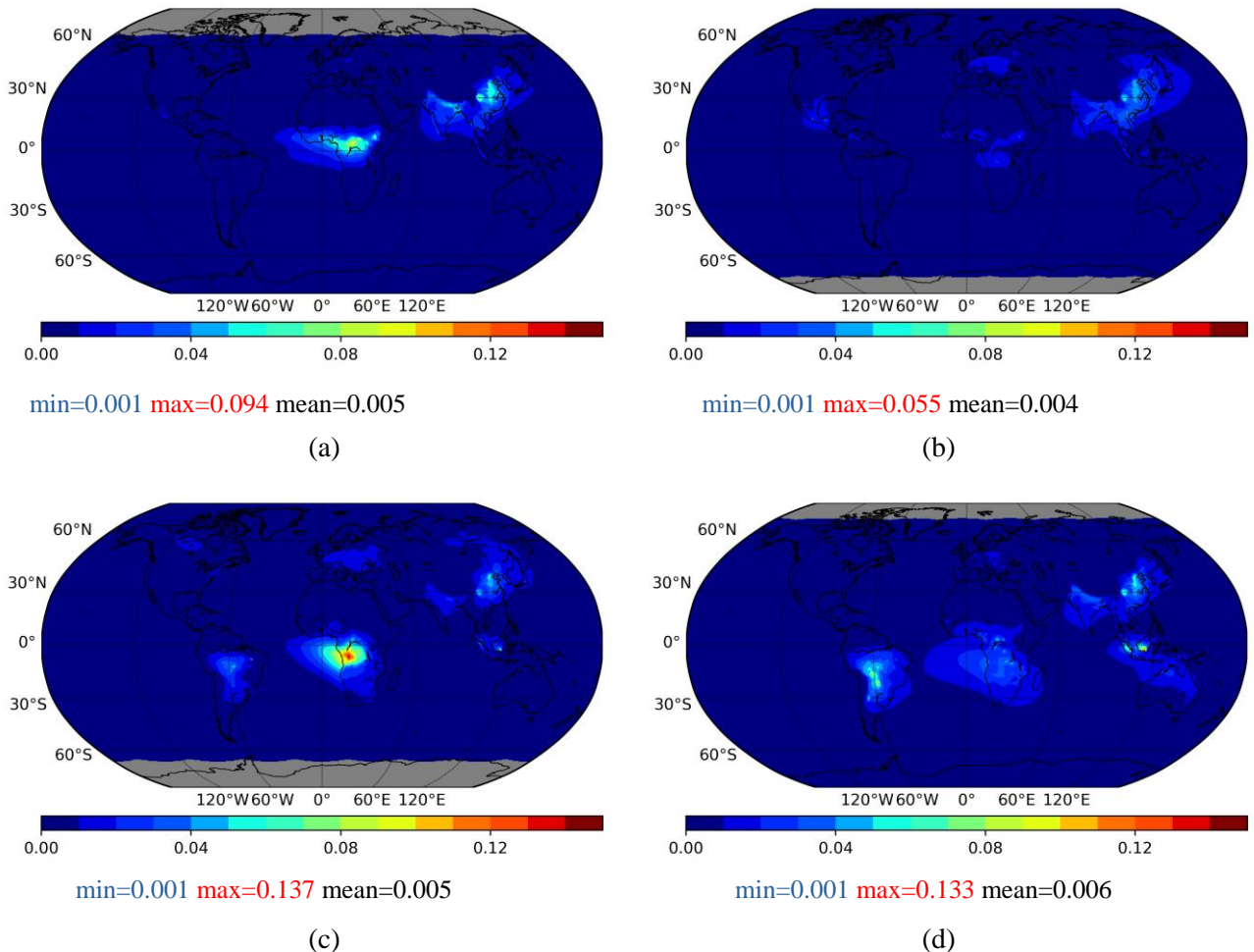


Figure S1vi. Mean seasonal (1980–2019) global distribution of MERRA-2 Optical Depth at the wavelength of 550 nm for black carbon particles. (a) winter, (b) spring, (c) summer, (d) autumn.

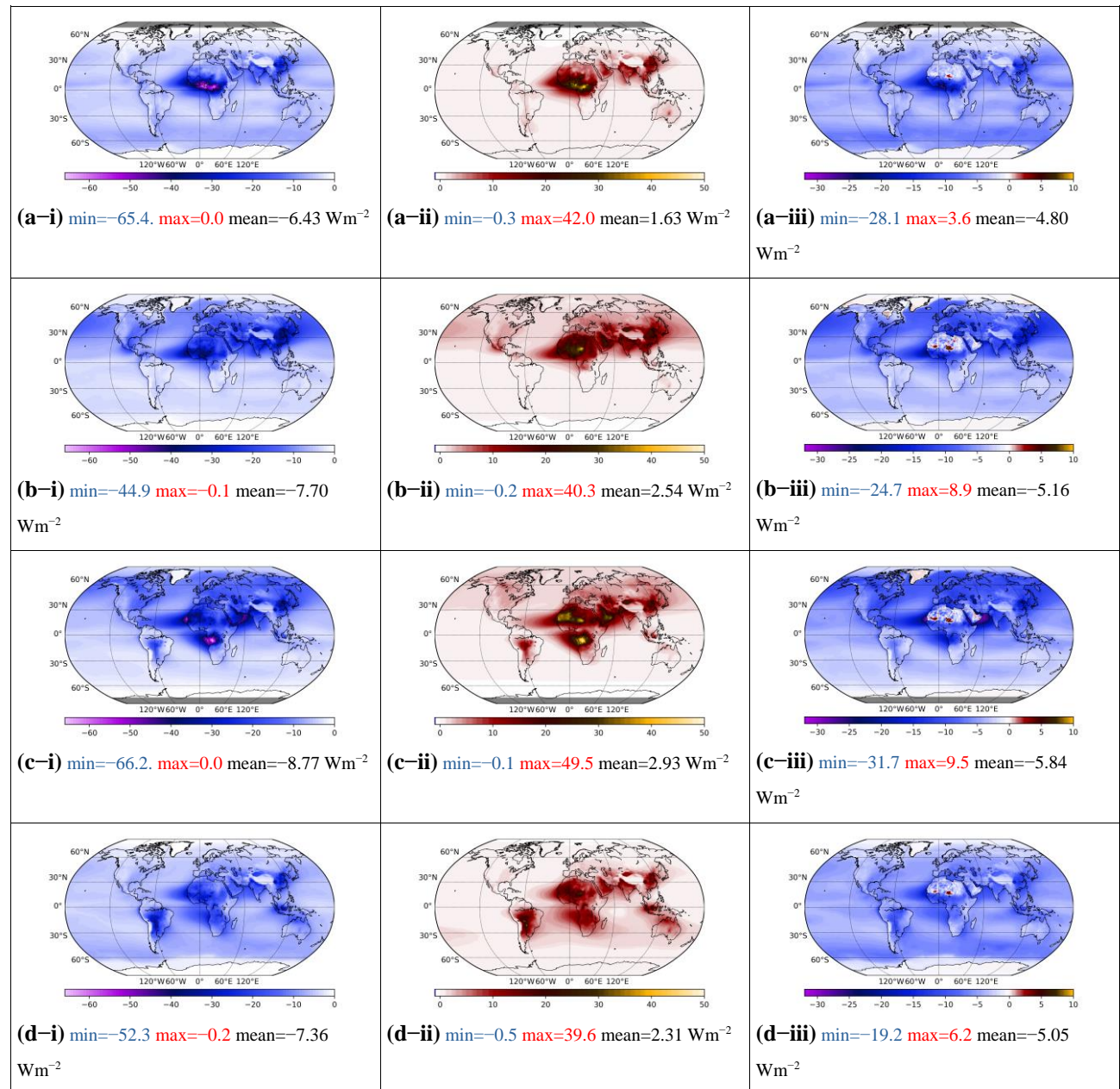


Figure S2. Mean (1980–2019) global distribution of total aerosol Direct Radiative Effects (i) at the Earth’s surface, (ii) within the Atmosphere and (iii) at the Top Of the Atmosphere, during (a) winter, (b) spring, (c) summer and (d) autumn.

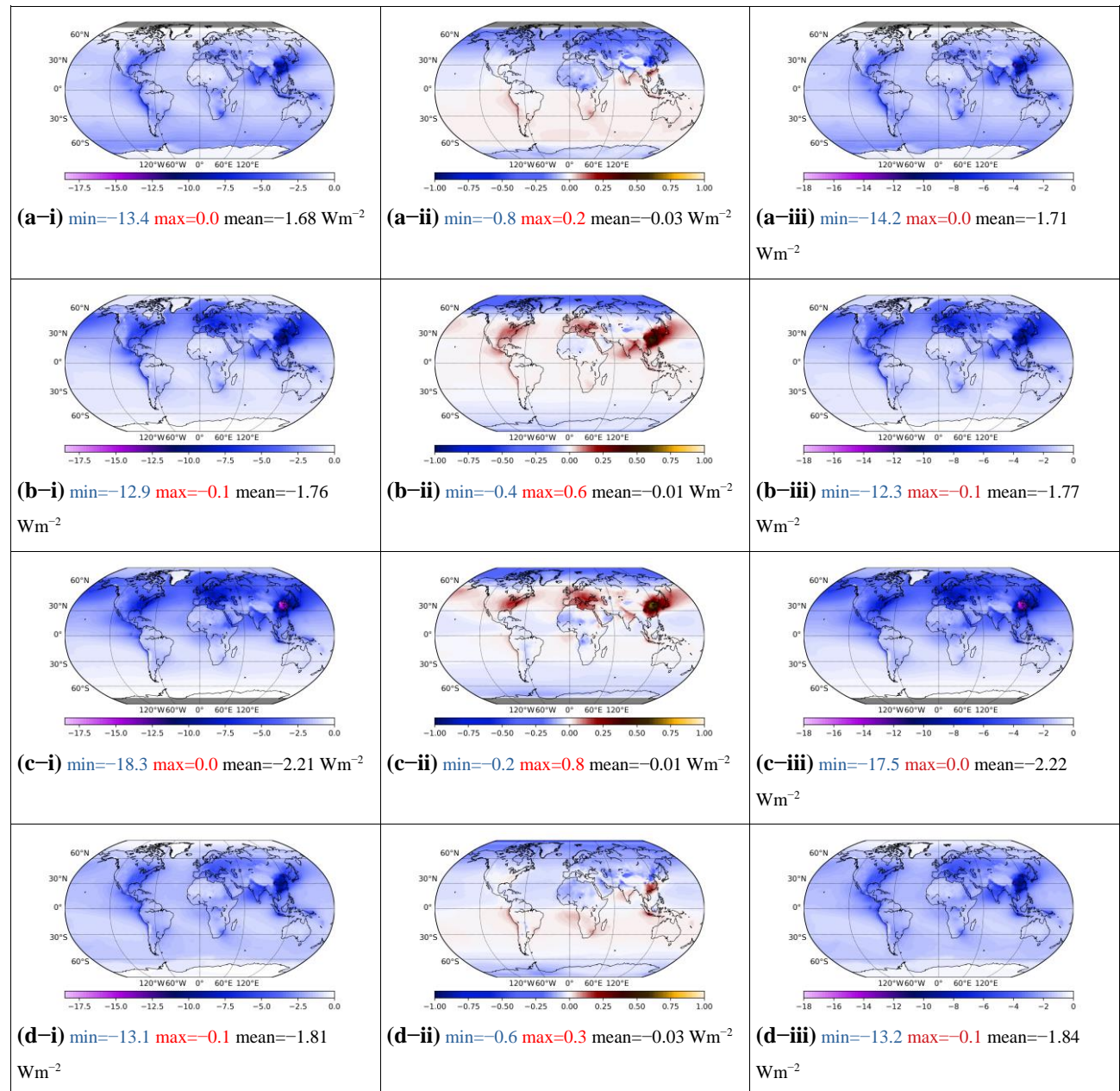


Figure S3. Mean (1980–2019) global distribution of sulfate aerosol Direct Radiative Effects (i) at the Earth's surface, (ii) within the Atmosphere and (iii) at the Top Of the Atmosphere, during (a) winter, (b) spring, (c) summer and (d) autumn.

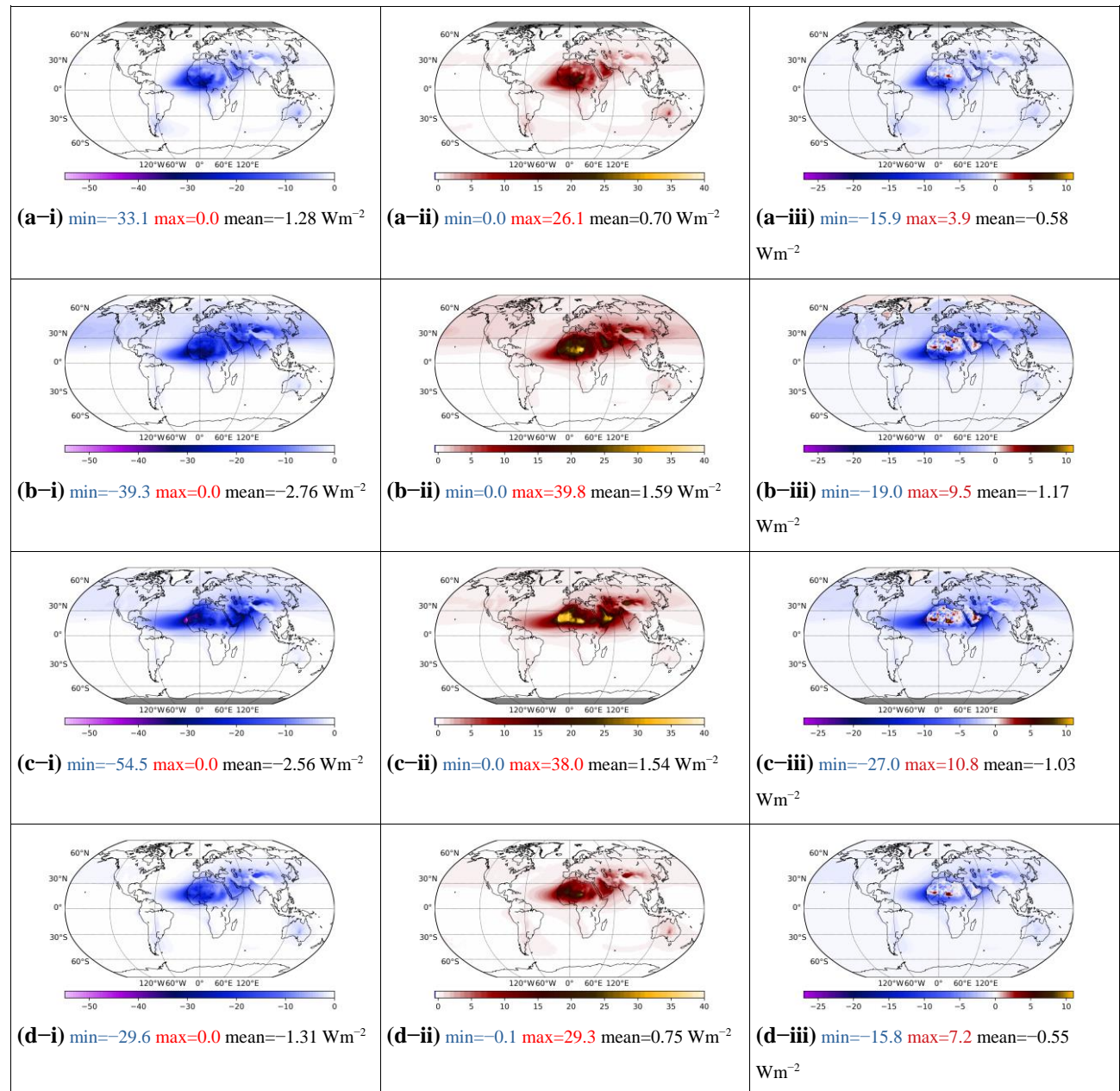


Figure S4. Mean (1980–2019) global distribution of dust aerosol Direct Radiative Effects (i) at the Earth’s surface, (ii) within the Atmosphere and (iii) at the Top Of the Atmosphere, during (a) winter, (b) spring, (c) summer and (d) autumn.

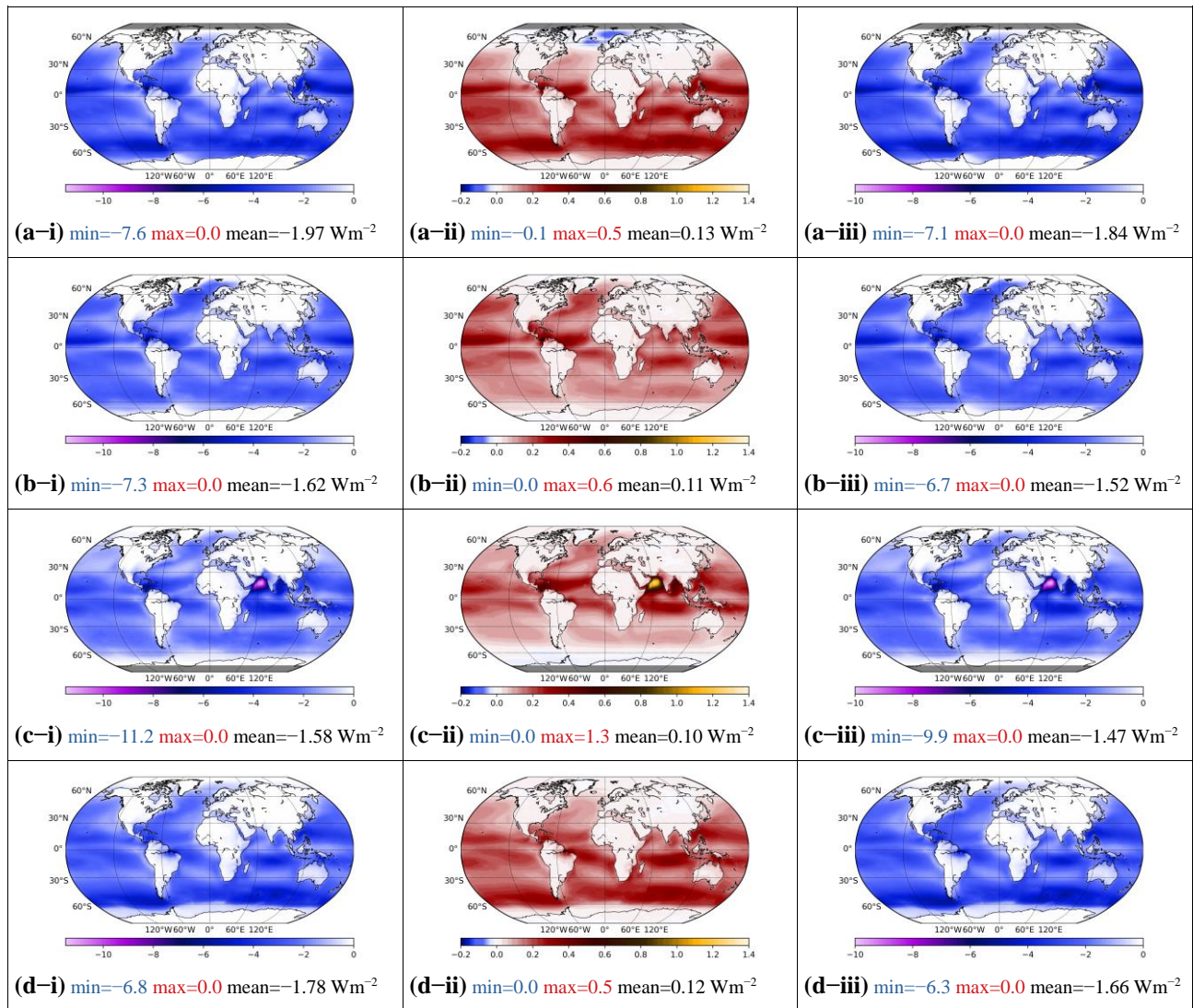


Figure S5. Mean (1980–2019) global distribution of sea salt aerosol Direct Radiative Effects (i) at the Earth's surface, (ii) within the Atmosphere and (iii) at the Top Of the Atmosphere, during (a) winter, (b) spring, (c) summer and (d) autumn.

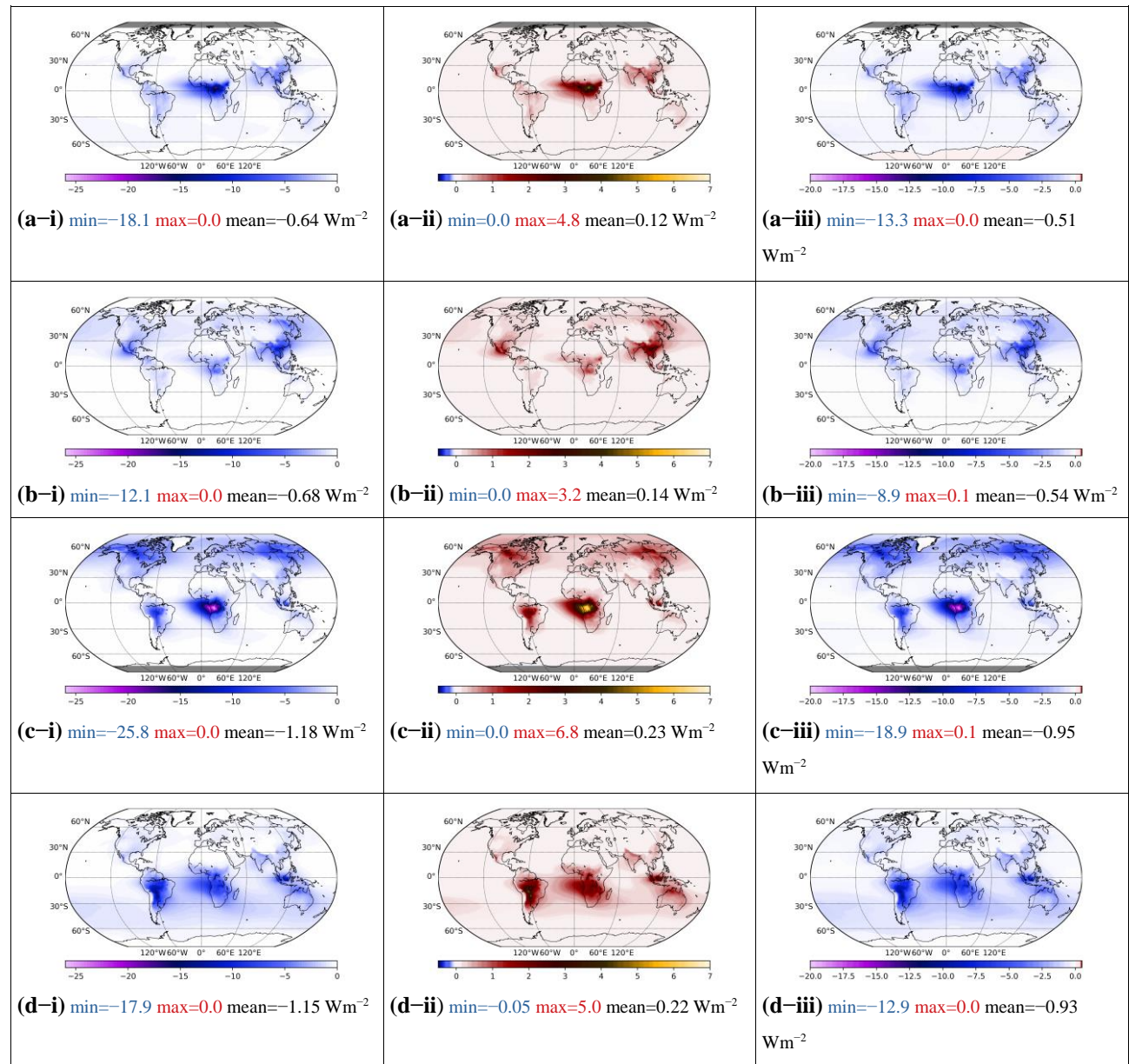


Figure S6. Mean (1980–2019) global distribution of organic carbon aerosol Direct Radiative Effects (i) at the Earth's surface, (ii) within the Atmosphere and (iii) at the Top Of the Atmosphere, during (a) winter, (b) spring, (c) summer and (d) autumn.

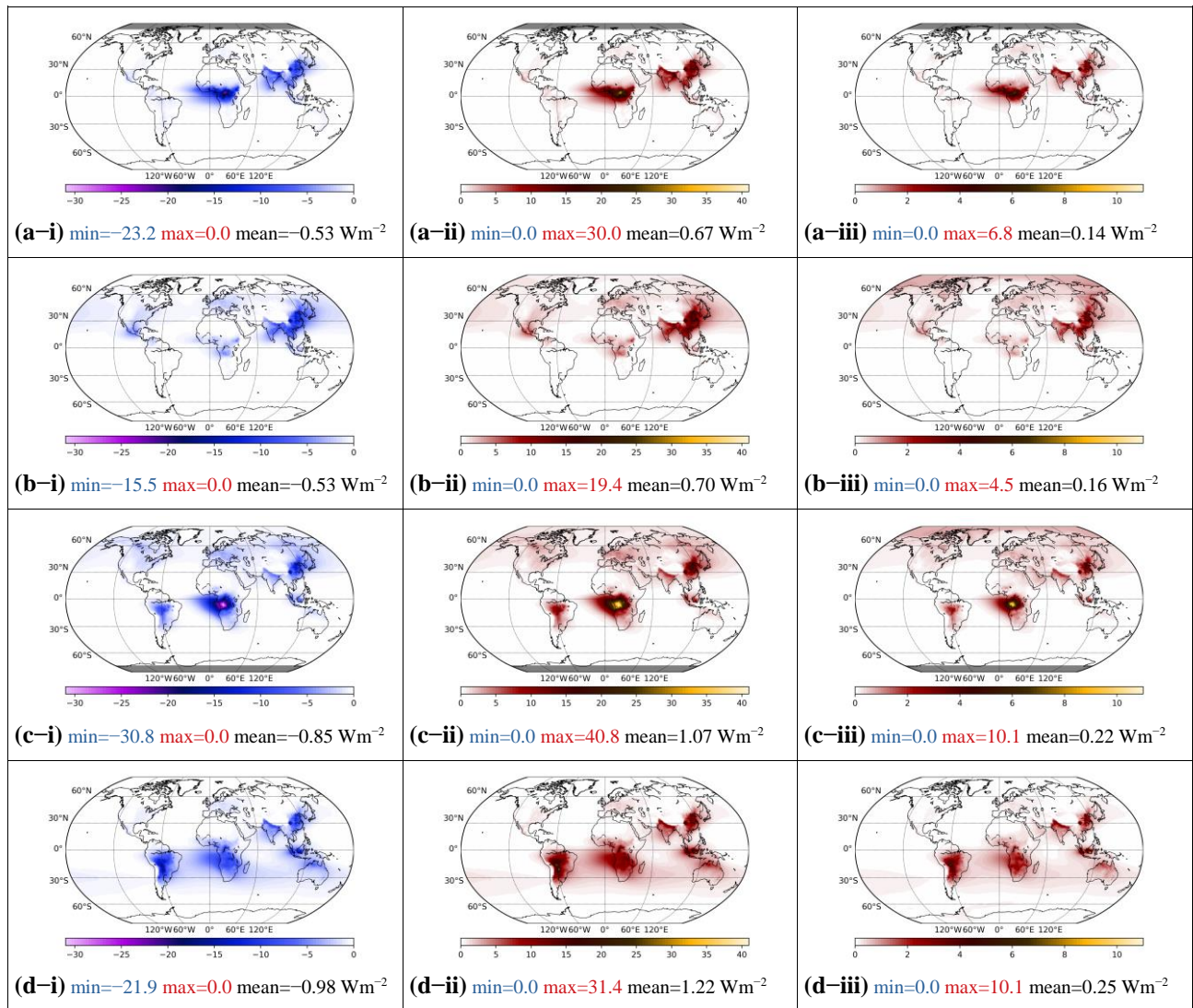


Figure S7. Mean (1980–2019) global distribution of black carbon aerosol Direct Radiative Effects (i) at the Earth's surface, (ii) within the Atmosphere and (iii) at the Top Of the Atmosphere, during (a) winter, (b) spring, (c) summer and (d) autumn.

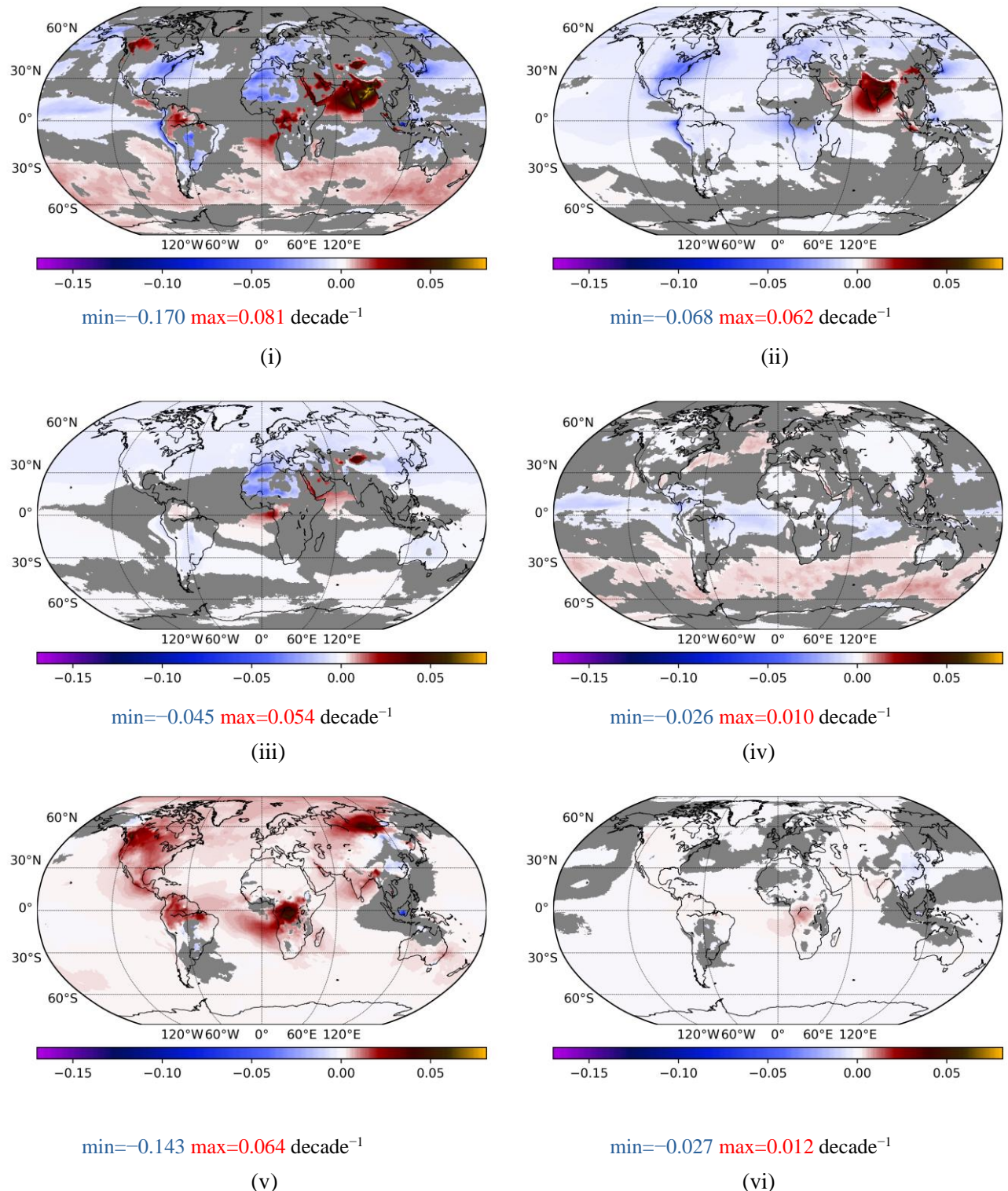
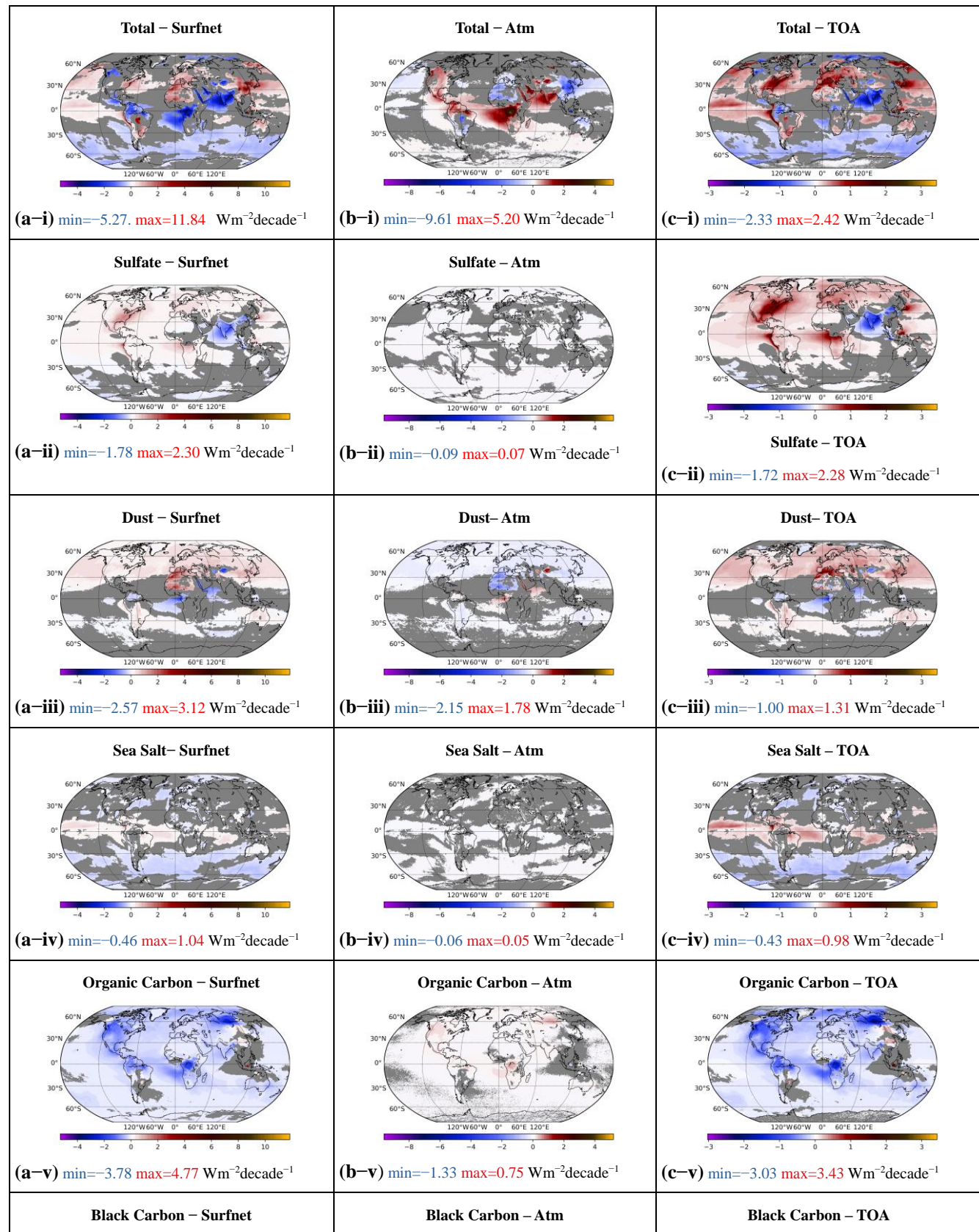


Figure S8. Slopes of deseasonalized MERRA-2 Optical Depth anomalies at the wavelength of 550 nm, over the period 2001–2019, for: (i) total aerosol load, (ii) sulfate, (iii) dust, (iv) sea salt, (v) organic carbon and (vi) black carbon particles. Only $0.5^\circ \times 0.625^\circ$ cells where trends are statistically significant at a 95% confidence level are shown. (units are decade⁻¹)



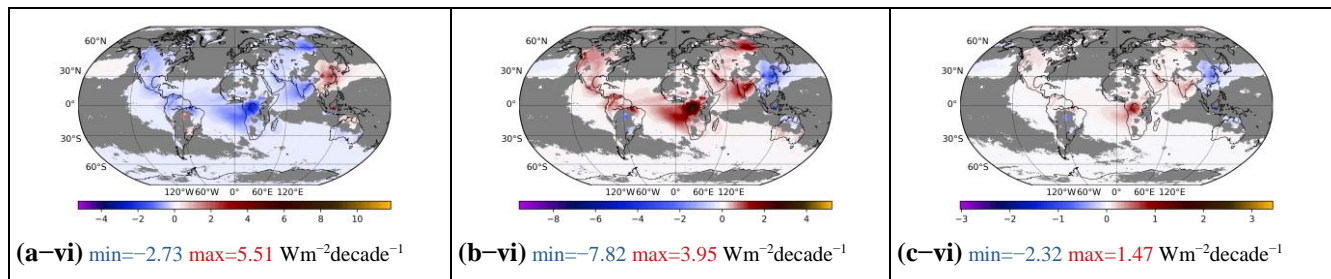


Figure S9. Slopes of deseasonalized Direct Radiative Effects anomalies over the period 2001–2019: (a) at the Earth’s surface, (b) within the Atmosphere and (c) at the Top Of the Atmosphere. (i) total aerosol load, (ii) sulfate, (iii) dust, (iv) sea salt, (v) organic carbon and (vi) black carbon particles. Only $0.5^\circ \times 0.625^\circ$ cells where trends are statistically significant at a 95% confidence level are shown. (units are $\text{Wm}^{-2}\text{decade}^{-1}$).

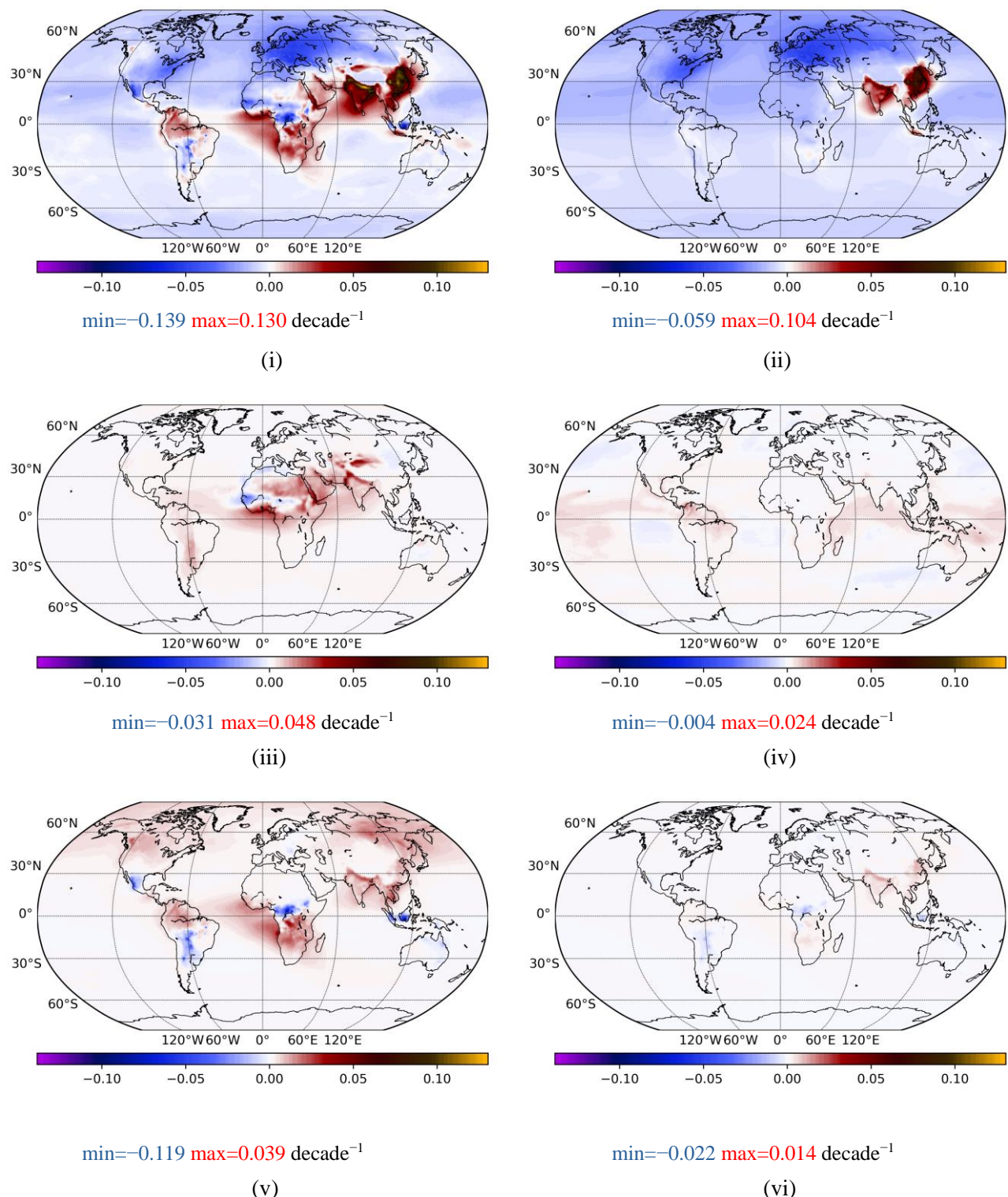
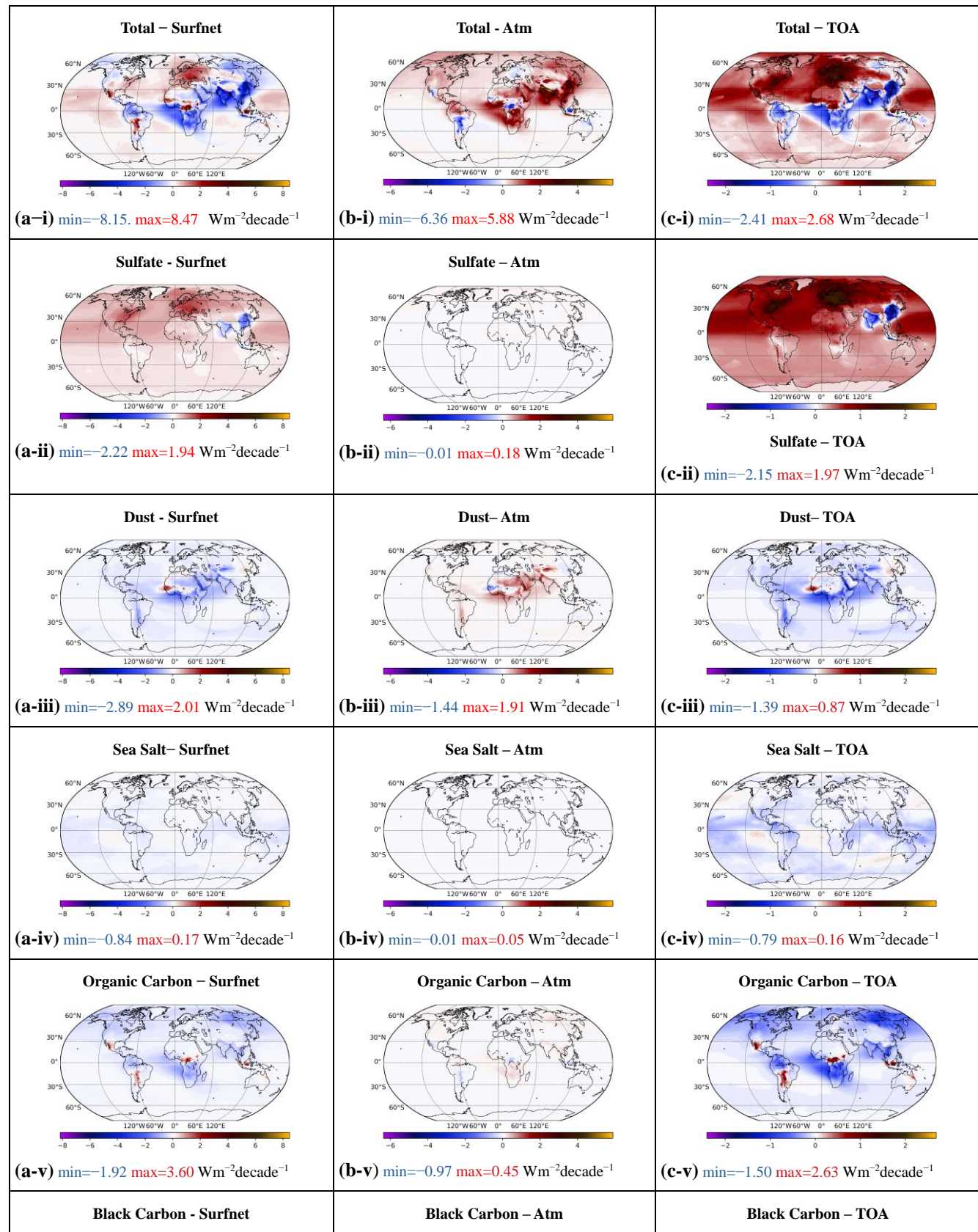


Figure S10. Slopes of deseasonalized MERRA-2 Optical Depth anomalies at the wavelength of 550 nm, over the period 1980–2019, for: (i) total aerosol load, (ii) sulfate, (iii) dust, (iv) sea salt, (v) organic carbon and (vi) black carbon particles. Only $0.5^\circ \times 0.625^\circ$ cells where trends are statistically significant at a 95% confidence level are shown. (units are decade⁻¹)



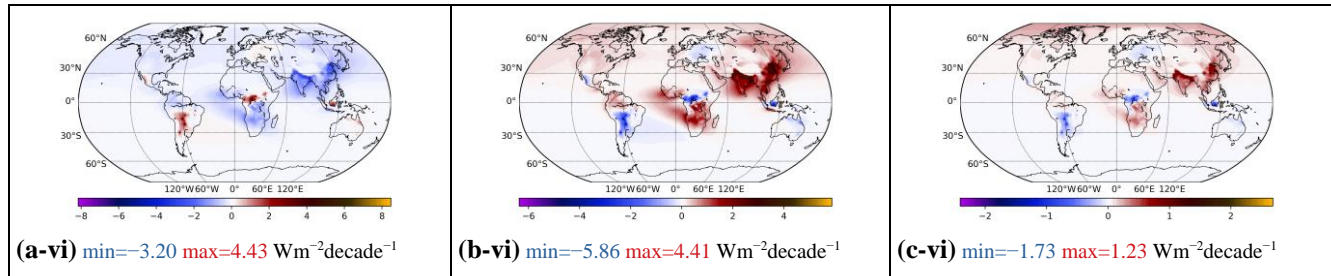


Figure S11. Slopes of deseasonalized Direct Radiative Effects anomalies over the period 1980-2019: (a) at the Earth's surface, (b) within the Atmosphere and (c) at the Top Of the Atmosphere. (i) total aerosol load, (ii) sulfate, (iii) dust, (iv) sea salt, (v) organic carbon and (vi) black carbon particles. (units are $\text{Wm}^{-2}\text{decade}^{-1}$)

Table S1. Decadal total aerosol AOD and DREs (in Wm^{-2}) over: the globe, the North and South Hemispheres, global land and global ocean areas and 5 selected world regions (Saharan and Arabian Deserts, Southern Africa, India, East Asia and Mediterranean).

		1980–1989	1990–1999	2000–2009	2010–2019
Global	DRE surface	−7.139	−7.792	−7.651	−7.671
	DRE atmosphere	1.973	2.010	2.686	2.745
	DRE TOA	−5.166	−5.781	−4.965	−4.926
	AOD	0.137	0.150	0.136	0.136
Northern Hemisphere	DRE surface	−9.494	−9.819	−10.203	−10.084
	DRE atmosphere	2.891	2.952	4.104	4.115
	DRE TOA	−6.603	−6.867	−6.099	−5.969
	AOD	0.179	0.186	0.175	0.172
Southern Hemisphere	DRE surface	−4.800	−5.778	−5.116	−5.275
	DRE atmosphere	1.061	1.075	1.277	1.384
	DRE TOA	−3.739	−4.704	−3.839	−3.890
	AOD	0.095	0.116	0.098	0.100
Global Land	DRE surface	−9.448	−9.908	−10.495	−10.481
	DRE atmosphere	4.142	4.275	5.371	5.428
	DRE TOA	−5.306	−5.633	−5.124	−5.053
	AOD	0.174	0.184	0.175	0.174
Global Ocean	DRE surface	−6.101	−6.840	−6.372	−6.408
	DRE atmosphere	0.998	0.992	1.479	1.539
	DRE TOA	−5.103	−5.848	−4.893	−4.869
	AOD	0.120	0.135	0.119	0.119
Saharan-Arabian Deserts	DRE surface	−17.531	−18.022	−18.876	−18.749
	DRE atmosphere	12.439	12.585	14.295	14.184
	DRE TOA	−5.092	−5.437	−4.581	−4.565
	AOD	0.325	0.341	0.338	0.335
Southern Africa	DRE surface	−8.653	−11.052	−12.641	−13.556
	DRE atmosphere	4.457	5.724	6.973	7.835
	DRE TOA	−4.195	−5.328	−5.668	−5.721
	AOD	0.131	0.164	0.178	0.184
India	DRE surface	−13.025	−14.221	−20.898	−22.827
	DRE atmosphere	5.346	5.768	10.916	11.690
	DRE TOA	−7.679	−8.453	−9.981	−11.138
	AOD	0.206	0.230	0.316	0.357
East Asia	DRE surface	−15.778	−17.695	−23.524	−22.248
	DRE atmosphere	6.235	7.026	11.544	10.111
	DRE TOA	−9.544	−10.669	−11.980	−12.137
	AOD	0.264	0.303	0.388	0.389

Mediterranean	DRE surface	−13.012	−11.916	−11.792	−10.805
	DRE atmosphere	4.411	3.915	5.031	4.655
	DRE TOA	−8.601	−8.002	−6.761	−6.151
	AOD	0.232	0.215	0.189	0.174